PHYSICAL REVIEW B **70**, 161103(R) (2004)

Evolution of local electronic states from a metal to a correlated insulator in a $NiS_{2-x}Se_x$ solid solution

K. Iwaya,[1,3] Y. Kohsaka,[2] S. Satow,[2] T. Hanaguri,[1,3] S. Miyasaka,[4] and H. Takagi[1,2,3]
[1]*RIKEN (The Institute of Physical and Chemical Research), Wako, Saitama 351-0198, Japan*
[2] *Department of Advanced Materials Science, The University of Tokyo, Kashiwa, Chiba 277-8651, Japan*
[3]*CREST, Japan Science and Technology Agency, Kawaguchi, Saitama 332-0012, Japan*
[4]*Department of Applied Physics, The University of Tokyo, Tokyo 113-8656, Japan*
(Received 7 June 2004; published 20 October 2004)

The evolution of local electronic states in $NiS_{2-x}Se_x$ pyrite as a bandwidth-controlled metal-insulator transition (MIT) approached from the metallic side is explored by scanning tunneling microscopy/spectroscopy (STM/STS). Atomically resolved images of Se/S zigzag chains are observed on top of the cubic (100) surface, and a narrowing of the quasiparticle band near the Fermi level is clearly identified in tunneling spectra. In marked contrast to MIT's control by doping, the local electronic states are found to be spatially homogeneous even in the vicinity of the MIT.

DOI: 10.1103/PhysRevB.70.161103 PACS number(s): 71.30.+h

The Mott metal-insulator transition (MIT), due to strong electron correlations, has been one of the major topics in condensed matter physics for many years.[1] Such MIT's can be driven by the control of two parameters: the strength of electron correlation U/W, and the band filling n. Here, W is the bandwidth and U is the on-site Coulomb interaction between electrons, respectively. The discovery of high temperature superconductivity in layered cuprates that has stimulated many attempts to describe the evolution of electronic states as a Mott insulator is approached by varying the band filling (doping). Recently the importance of real space physics has been emphasized in filling-controlled MIT's. It has been argued that a spatial segregation of doped carriers occurs as a consequence of the competition between the itinerancy of the carriers and the magnetic background. Nanoscale electronic inhomogeneity is indeed observed in real space by scanning tunnel microscopy/spectroscopy (STM/STS), which has been often discussed in terms of electronic phase separation.[2–7]

MIT's driven by a change in U/W are described as "bandwidth controlled." We naively expect less pronounced electronic inhomogeneity in the vicinity of MIT due to the absence of doped carriers and charged impurities as compared with the filling-controlled MIT. However, this naive expectation has never been checked experimentally as a function of U/W using a spatially resolved probe. This is largely because of the lack of a suitable model system for such a study. In this communication, we identify $NiS_{2-x}Se_x$ as an ideal system for studying the evolution of local electronic states across a bandwidth-controlled MIT by STM/STS. Atomically resolved topographic images were obtained. The narrowing of the quasiparticle bands near the Fermi level E_F was clearly observed in STS spectra for compositions approaching the MIT. Electronic inhomogeneity in the vicinity of the MIT was far less pronounced than in the filling-controlled case.

The Ni-pyrite system, $NiS_{2-x}Se_x$, has a rich phase diagram with different competing magnetic order parameters, as shown in Fig. 1(a).[8] The end member NiS_2 is a charge-transfer insulator[9,10] and crystallizes in a pyrite structure in which Ni and S_2 form a NaCl-type lattice [Fig. 1(b)]. As x (Se concentration) increases, $NiS_{2-x}Se_x$ undergoes an antiferromagnetic insulator (AFI) to an antiferromagnetic metal (AFM) transition at around $x=0.45$, essentially due to an increase of the electronic bandwidth.[11,12] The AFM phase exists in the range $0.45<x<1.0$ at low temperatures and a

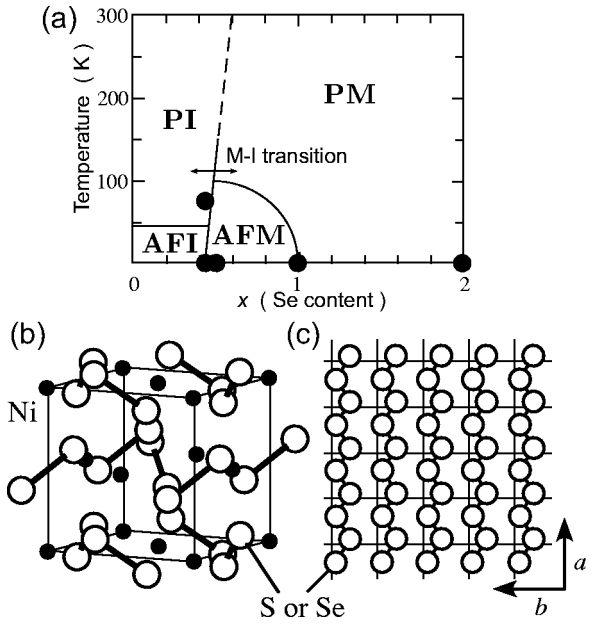

FIG. 1. (a) Schematic phase diagram of $NiS_{2-x}Se_x$ solid-solution Ref. 10. (PI, paramagnetic insulator phase; AFI, antiferromagnetic insulator phase; PM, paramagnetic metal phase; AFM, antiferromagnetic metal phase). Filled circles ($x=0.45$, 0.5, 1.0, 2.0) correspond to the compositions investigated in this study. (b) The crystal structure of the $NiS_{2-x}Se_x$ solid solution. Ni and $(S,Se)_2$ pairs form a NaCl-type structure and each $(S,Se)_2$ pair is aligned parallel to another one of the four $\langle 111 \rangle$ axes. (c) The structure of uppermost (S,Se) planes of the (100) surface. Zigzag chains of chalcogen atoms (S or Se) are running along the cubic a axis. The solid lines correspond to the sublattice of nickel atoms.

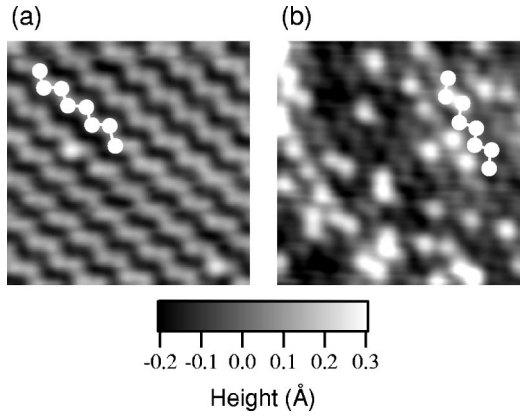

FIG. 2. STM topographic images of $NiS_{2-x}Se_x$ taken at $T=4.7$ K (47 Å$\times$47 Å). The measurement was performed with a constant current mode (bias voltage $V_s=500$ mV, tunneling current $I_t\sim100$ pA). (a) $x=2.0$ (paramagnetic metal phase), (b) $x=0.5$ (a sample in the vicinity of the MIT).

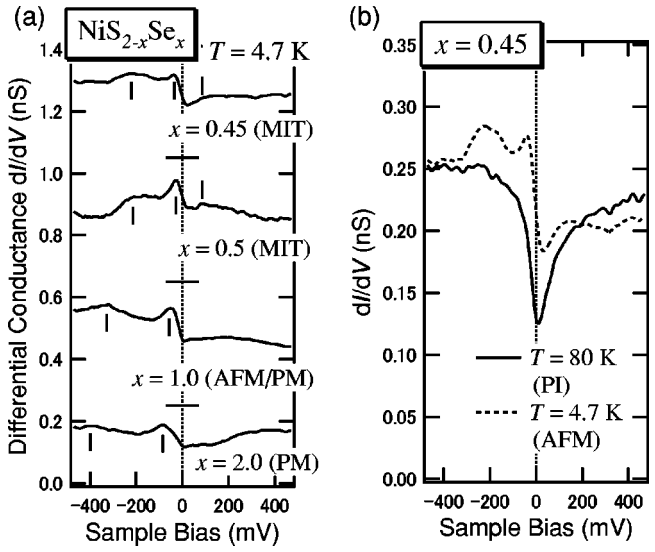

FIG. 3. The spatially averaged differential conductance dI/dV spectra for $NiS_{2-x}Se_x$. (a) Se content x dependence of averaged dI/dV spectra at 4.7 K ($x=0.45$, 0.5, 1.0, 2.0). Each spectrum, except for $x=2.0$, is shifted vertically for clarity. (b) Temperature variation of the averaged dI/dV spectra for $NiS_{1.55}Se_{0.45}$ ($x=0.45$) from AFM to PI phase.

paramagnetic metal (PM) phase exists in the range $x>1.0$ over the whole temperature range. NiSSe ($x=1.0$) is located at a quantum critical point (QCP) between the AFM and PM phase. This system is unique for the study of MIT's in that the bandwidth can be tuned continuously by chemical substitution without apparent change of structural symmetry.[13] In addition, since this system shows good cleavage along the (100) plane, it can be prepared with an atomically clean and flat surface, which is suitable for high resolution STM/STS measurements.

The single crystals of $NiS_{2-x}Se_x$ used in this study, grown by a vapor transport technique, were taken from the same batch used in the previous study.[14] We measured several samples with different Se concentrations, including $x=0.45$, 0.5 (samples in the vicinity of the MIT on the metallic side), $x=1.0$ (AFM-PM phase boundary), and $x=2.0$ (PM phase). These samples were cleaved along the (100) plane at room temperature in ultrahigh vacuum (UHV) conditions and then transferred to the low-temperature STM immediately after cleavage. Differential conductance dI/dV spectra, which are proportional to the local density of states (LDOS), were obtained by numerical differentiation of I-V curves. The STM tips used in this study, a chemically etched tungsten (111)-oriented single crystal, were cleaned and sharpened in a controlled manner at room temperature by field evaporation using field ion microscopy.

Figure 2(a) shows a typical STM image of the end member $NiSe_2$ ($x=2.0$), which is a paramagnetic metal. An atomic image with parallel zigzag chains is clearly observed. Considering the different possible (100) surface structures, we conclude that the uppermost Se plane gives rise to the zigzag chains as shown in Fig. 1(c). From this, we can infer a cubic lattice constant of $\sim$6.0 Å, which agrees well with values previously found by x-ray diffraction.[15]

In the S substituted crystals, the Se—S solid solution could be clearly resolved on an atomic scale. Figure 2(b) shows the STM image of an $x=0.5$ sample (close to the MIT boundary) and the zigzag structure is still observed. In contrast to $x=2.0$, there are two kinds of atoms (white and gray dots), which are randomly distributed. The ratio of the white and the gray dots is roughly 1:3, which very likely indicates the two distinct dots correspond to Se and S atoms, respectively. The difference in height between white and gray atoms is of the order of 0.1 Å, comparable to the difference of ionic radius between S and Se. Furthermore, we found that the ratio of white dots systematically increases with Se substitution. From these considerations, we identify the white dots as Se atoms and the gray dots as the S atoms.

We did not observe any superstructure in this system. The presence of metal-like surface layers in $x=0$ and 0.4 (bulk insulating phase) has been reported and the presence of substantial amount of S vacancies at the surface was suggested.[16,17] Watanabe *et al.* argued that the increase of S/Se vacancies with x dominates the MIT in this system due to the increase of hole concentration.[18] In contrast to these proposals, however, appreciable number of S vacancies were not seen independent of the Se content x in the STM images.

We have performed tunneling spectroscopy on these well characterized surfaces to explore the evolution of electronic states as the Se content is decreased and the system approaches the MIT. In Fig. 3(a), the averaged tunneling conductance spectra taken at 4.7 K for crystals with various Se contents are summarized. We find several characteristic features: (1) A well-defined two peak structure below E_F in all samples. (2) As x approaches the MIT at $x\sim0.45$, the two peaks below E_F become sharper and gradually shift toward E_F. (3) A broad peak above E_F, which shows a similar evolution as those below E_F.[19] In figure 3(b), the variation of spectra with temperature for $x=0.45$ is shown. In $x=0.45$, the system undergoes a temperature induced transition from AFM to PI ($T=80$ K). In accord with the transition, the dI/dV spectrum clearly shows the suppression of low energy DOS at high temperature, suggesting the opening of gap. The

opening of gap associated with MIT was previously observed by tunneling spectroscopy.[20] These distinct correlations between the bulk properties and dI/dV spectrum indicates that our measurements probe the bulk properties of this compound.

The end member NiS_2 is a charge transfer insulator with a charge transfer gap of 1 eV between S/Se nonbonding $p\pi$ bands and Ni $3d$ e_g upper Hubbrad bands.[21] When the system becomes metallic through an increase of bandwidth, quasiparticle states are believed to emerge which are primarily of Ni $3d$ e_g and S/Se p characters. Because of the degeneracy of Ni $3d$ e_g bands and their hybridization with S/Se nonbonding $p\pi$ bands, the quasiparticle bands near E_F can be expected to have a complicated structure, which will manifest itself in multiple peaks in the DOS. We do indeed observe such structure, but due to the lack of detailed band structure calculations, we are not able to assign DOS peaks to partial band. The quasiparticle bands formed around E_F are strongly renormalized as one approaches the MIT, which manifests itself as an enhancement of specific heat coefficient γ. Indeed, previous work by Miyasaka *et al.* found an enhancement of γ by a factor 5 from $x=2.0$ (PM) to $x=1.0$ (at QCP).[14] The observation (2) clearly indicates that the quasiparticle bands near E_F tend to narrow as the system approaches the MIT. This is consistent with the picture suggested by specific heat measurements. The systematic evolution of coherent quasiparticle bands near E_F in the vicinity of MIT is also in good agreement with the previous angle-resolved photoemission spectroscopy (ARPES) study.[21,22]

From the bulk measurements, there is a sharp contrast in the approach to an insulator between the AFM and the PM phases. The specific heat coefficient γ has a peak around $x=1.0$ (QCP) and shows a decrease to an insulating state in the antiferromagnetic metal phase.[14] In the AFM phase, a band splitting due to the presence of long-range magnetic ordering is anticipated, which will create a small pseudogap and hence results in the decrease of γ. In accord with this picture, a substantial decrease of carrier density is inferred from the Hall coefficient R_H and the residual resistivity ρ_0, which can be understood in terms of the formation of a small Fermi surface due to band splitting. The evidence for such a pseudogap in the AFM phase is immediately not evident in the tunneling spectra of AFM samples with $x=0.45-1.0$. On closer examination, however, we notice that there exists a tiny DOS dip right above E_F, which is reminiscent of the pseudogap. This rather weak pseudogapsignature may not be surprising, since the decrease in γ from $x=1.0$ (QCP) to $x=0.5$ is as small as 30%.

Finally, we discuss the spatial variation of electronic states, which has been a subject of longstanding debate in the physics of filling-controlled MIT system, including high-T_c superconducting cuprates and colossal-magnetoresistance manganites. In these well studied compounds, a nanoscale corrugation of the topographic image has been observed by a number of groups.[4,6] Since the tunneling current is exponentially related to the tip-sample distance and is also proportionally related to the integrated LDOS, the corrugation of a topographic image taken by the constant current mode may originate not only from the topology but also from the LDOS variation. In these filling controlled MIT systems, namely

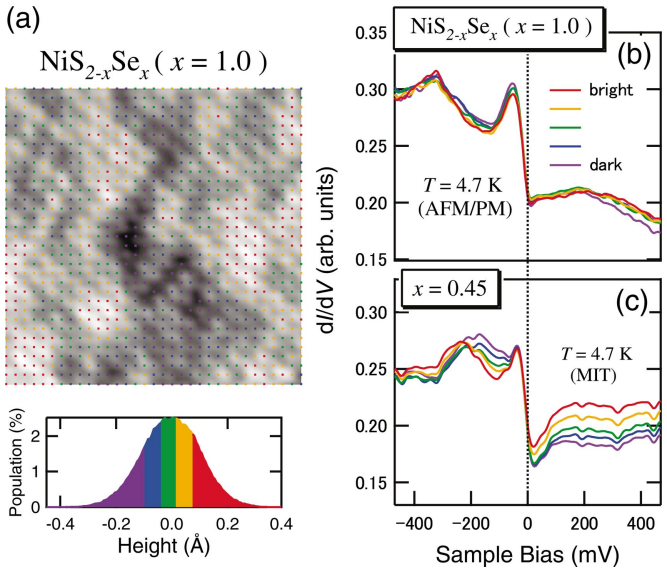

FIG. 4. (Color) Real-space variation of tunneling spectra for $NiS_{2-x}Se_x$. (a) STM topographic image of $x=1.0$ (AFM-PM phase boundary). A nanoscale corrugation is superposed on atomically resolved zigzag chains (94 Å×94 Å, $T=4.7$ K, $V_s=500$ mV, $I_t \sim 100$ pA). The superimposed dots (32×32 points) indicate the locations where tunneling spectra are measured. Five different colors are assigned to these dots according to the apparent height in the image. (b) Averaged differential conductance spectra for $x=1.0$ (AFM-PM phase boundary) at each apparent height in (a). (c) Apparent height dependence of averaged dI/dV spectra for $x=0.45$ at $T=4.7$ K (near the MIT), obtained in the same way as (b).

doped Mott insulators, the shape of tunneling spectra shows a real-space variation with a clear correlation to the apparent height in the topographic images, and it is widely believed that the corrugation is dominated by the real-space variation of local electronic states.

The real-space physics of the bandwidth-controlled system, $NiS_{2-x}Se_x$, appears to be very different. In the topographic images of the end member $NiSe_2$ ($x=2.0$), we do not observe any structure except for the zigzag lattice. In accordance with this, the conductance spectra show no spatial variation indicating homogeneous electronic states in this sample. As S is substituted for Se (i.e., as we approach the insulator), a nanoscale corrugation shows up in the zigzag S/Se planes. A typical example for $x=1.0$ crystal (at the AFM-PM critical point) is illustrated in Fig. 4(a), which shows approximately ~0.3 Å distribution of apparent height about ~100 Å scale. At first glance, this reminds us of the electronic inhomogeneity in filling-controlled systems. However, this corrugation is not electronic in origin but essentially a topographic effect. In Fig. 4(b), the conductance spectra for the regions with different heights are compared. The spectra from different regions agree with each other remarkably as well as $NiSe_2$. This clearly indicates the absence of spatial variation in local electronic states, although this sample is close to a correlated insulator and the specific coefficient γ is enhanced by a factor of 5 as compared to $NiSe_2$. The observed corrugation is perhaps associated with a spatial variation of chemical pressure inherent to solid-solution systems. Only around $x=0.45, 0.5$ right at the metallic side of

the MIT, we do eventually find a spatial variation of the conductance spectrum as demonstrated in Fig 4(c). Even in this $x=0.45$ sample, however, LDOS peaks are always present and the peak positions show only minute change. In particular, the peak right below E_F, which is responsible for MIT, does not show any spatial variation within our energy resolution. Although not shown here, similar behavior was observed in $x=0.5$. In the case of high-T_c cuprates, the disappearance of the superconducting coherence peak and/or a characteristic DOS kink has been observed in the position-dependent dI/dV curves.[4–6] Therefore, the observed electronic inhomogeneity in $x=0.45$, 0.5 is considerably less pronounced than in lightly doped high temperature superconductors. This marked contrast suggests that the carrier doping promotes the occurrence of nanoscale electronic inhomogeneity in filling-controlled systems including cuprates and manganites. This is probably because of the deviation from the integer filling and the presence of charged dopants. The contrast between filling and bandwidth-controlled MIT is therefore worthy for further exploration.

In conclusion, we report the observation of atomic lattice and systematic spectroscopy measurements for the $NiS_{2-x}Se_x$ solid solution which undergoes a bandwidth-controlled metal-insulator transition by the substitution of S with Se. Our spectroscopic measurements for the samples with different Se concentrations reveal that a narrow band develops near E_F as the system approaches the MIT, and that $NiS_{2-x}Se_x$ has almost spatially homogeneous electronic states even in the vicinity of the MIT. In particular, the latter feature makes clear contrast with filling-controlled MIT systems in which electronic inhomogeneity is observed even in the metallic region. We therefore conclude that the real-space physics of filling and bandwidth-controlled MIT systems is essentially different.

We thank K. Kitazawa and A. Maeda for encouragement of this research and N. Shannon for critical reading of the manuscript.

[1] M. Imada, A. Fujimori, and Y. Tokura, Rev. Mod. Phys. **70**, 1039 (1998).

[2] Ch. Renner, G. Aeppll, B.-G. Kim, Yeong-Ah Soh, and S.-W. Cheong, Nature (London) **416**, 518 (2002).

[3] M. Fäth, S. Freisem, A. A. Menovsky, Y. Tomioka, J. Aarts, and J. A. Mydosh, Science **285**, 1540 (1999).

[4] S. H. Pan, J. P. O'Neal, R. L. Badzey, C. Chamon, H. Ding, J. R. Engelbrecht, Z. Wang, H. Eisaki, S. Uchida, A. K. Gupta, K.-W. Ng, E. W. Hudson, K. M. Lang, and J. C. Davis, Nature (London) **413**, 282 (2001).

[5] K. M. Lang, V. Madhavan, J. E. Hoffman, E. W. Hudson, H. Eisaki, S. Uchida, and J. C. Davis, Nature (London) **415**, 412 (2002).

[6] Y. Kohsaka, K. Iwaya, S. Satow, T. Hanaguri, M. Azuma, M. Takano, and H. Takagi, Phys. Rev. Lett. **93**, 097004 (2004).

[7] Z. Wang, J. R. Engelbrecht, S. Wang, H. Ding, and S. H. Pan, Phys. Rev. B **65**, 064509 (2002).

[8] For a review, see J. A. Wilson, in *The Metallic and Nonmetallic State of Matter*, edited by P. P. Edwards and C. N. R. Rao (Taylor and Francis, London, 1985), pp. 215–261.

[9] A. Fujimori, K. Mamiya, T. Mizokawa, T. Miyadai, T. Sekiguchi, H. Takahashi, N. Môri, and S. Suga, Phys. Rev. B **54**, 16 329 (1996).

[10] In the AFI phase, a weak ferromagnetic phase at low temperature was observed. See, for example, Ref. 8.

[11] F. Gautier, G. Krill, M. F. Lapierre, P. Panissod, C. Robert, G. Czjzek, J. Fink, and H. Schmidt, Phys. Lett. **53A**, 31 (1975).

[12] S. Ogawa, J. Appl. Phys. **50**(3), 2308 (1979).

[13] J. A. Wilson and G. D. Pitt, Philos. Mag. **23**, 1297 (1971).

[14] S. Miyasaka, H. Takagi, Y. Sekine, H. Takahashi, N. Môri, and R. J. Cava, J. Phys. Soc. Jpn. **69**, 3166 (2000).

[15] P. Kwizera, M. S. Dresselhaus, and D. Adler, Phys. Rev. B **21**, 2328 (1980).

[16] T. Thio and J. W. Bennett, Phys. Rev. B **50**, 10 574 (1994).

[17] D. D. Sarma, S. R. Krishnakumar, E. Weschke, C. Schüßler-Langeheine, Chandan Mazumdar, L. Kilian, G. Kaindl, K. Mamiya, S.-I. Fujimori, A. Fujimori, and T. Miyadai, Phys. Rev. B **67**, 155112 (2003).

[18] H. Watanabe and S. Doniach, Phys. Rev. B **57**, 3829 (1998).

[19] We observed all the main features (1)–(3) in each spectrum before averaging.

[20] J. G. Rodrigo, S. Vieira, P. Somasundaram, J. M. Honig, F. A. Chudnovsky, and V. N. Andreev, Phys. Rev. B **58**, 10 256 (1998).

[21] A. Y. Matsuura, Z.-X. Shen, D. S. Dessau, C.-H. Park, T. Thio, J. W. Bennett, and O. Jepsen, Phys. Rev. B **53**, R7584 (1996).

[22] A. Y. Matsuura, H. Watanabe, C. Kim, S. Doniach, Z.-X. Shen, T. Thio, and J. W. Bennett, Phys. Rev. B **58**, 3690 (1998).